# Design Considerations for Single-Mode Microring Lasers Using Parity-Time-Symmetry

Hossein Hodaei, Absar U. Hassan, Jinhan Ren, William E. Hayenga, Mohammad-Ali Miri, Demetrios N. Christodoulides, and Mercedeh Khajavikhan

*(Invited Paper)*

***Abstract*—Coupled microring arrangements with balanced gain and loss, also known as parity-time symmetric systems, are investigated both analytically and experimentally. In these configurations, stable single-mode lasing can be achieved at pump powers well above threshold. This self-adaptive mode management technique is broadband and robust to small fabrication imperfections. The results presented in this paper provide a new avenue in designing mode selective chip-scale in-plane semiconductor lasers by utilizing the complex dynamics of coupled gain/loss cavities.**

***Index Terms*—Optical waveguides, ring lasers, semiconductor lasers.**

## I. Introduction

CONTROLING the modal content of laser cavities has been a long standing challenge in laser science and engineering [1]. This problem becomes particularly acute in semiconductor laser arrangements where the gain spectrum is broad and thus multimode operation is inevitable. Over the years, a number of schemes have been proposed to enforce single mode behavior in semiconductor laser systems. These include the use of external cavities [2], [3], intra-cavity periodic dispersive elements [4], as well as Vernier resonators [5], to mention a few. However, implementing such techniques can sometimes become exceedingly demanding in terms of fabrication and tuning, especially in micro-scale monolithically integrated lasers. Thus, devising alternative methods for mode management in integrated settings is of great importance.

Microring resonators exhibit several desirable features such as high Q-factors, small footprints, and simplicity of fabrication [6]. These qualities make them promising candidates for on-chip laser applications. However, despite their small size, semiconductor microrings tend to support several longitudinal modes with comparable quality factors. The ensuing multi-mode operation compromises the coherence and spectral purity of the laser, which in turn can cause power fluctuation and instability.

Manuscript received December 13, 2015; revised February 2, 2016 and February 4, 2016; accepted February 6, 2016. This work was supported in part by the NSF CAREER Award (ECCS-1454531), NSF (ECCS-1128520 and DMR-1420620), AFOSR (FA9550-14-1-0037), and ARO (W911NF-16-1-0013).

The authors are with the College of Optics and Photonics, University of Central Florida, Orlando, FL 32816, USA (e-mail: hodaei@knights.ucf.edu; absar.hassan@knights.ucf.edu; jinhan.ren@knights.ucf.edu; whayenga34@knights.ucf.edu; miri@knights.ucf.edu; demetri@creol.ucf.edu; mercedeh@creol.ucf.edu).

Color versions of one or more of the figures in this paper are available online at http://ieeexplore.ieee.org.

Digital Object Identifier 10.1109/JSTQE.2016.2537277

Recently, we have demonstrated that by pairing an active microring resonator with a lossy but otherwise identical partner, it is possible to enforce single mode operation even in the presence of strong mode competition [7]. At first glance, adding loss into a laser cavity may appear both counter-intuitive and detrimental. However, this perspective has largely changed due to recent theoretical and experimental studies showing that the presence of exceptional or phase transition points in systems with balanced gain and loss (parity-time (PT) symmetric) can be fruitfully utilized to attain a host of new behaviors and functionalities [7]–[27]. Thus far, this methodology has been explored in a number of laser studies where single mode lasing, a lower threshold, and an inverse pump dependence on output power have been demonstrated [7], [22]–[27].

In this paper, we review some of our recent activities and outline our design considerations in regard to single mode PT-symmetric microring lasers. Section II presents a brief introduction to PT-symmetry in photonics. In Section III, a coupled mode analysis is developed to study symmetry breaking and single mode operation in PT lasing systems. Section IV discusses the lasing threshold for PT lasers. Section V describes the methods used for implementing and characterizing such arrangements. Experimental results are presented in Section VI. Effects arising from deviation from exact PT-symmetry are analytically investigated in Section VII. Finally, Section VIII concludes the paper.

## II. PT-Symmetry in Optics

In 1998, it was shown that a wide class of non-Hermitian Hamiltonians can exhibit entirely real spectra provided that they commute with the parity-time (PT) operator [28]. To some extent, this counterintuitive result goes against the commonly held view that real eigenvalues are only associated with Hermitian observables. Starting from the aforementioned premise, one can directly show that a necessary (but not sufficient) condition for PT-symmetry to hold is that the complex potential involved in such a Hamiltonian should satisfy $V(x) = V^*(-x)$ [28]. In other words, the real part of the complex potential must be an even function of position, while the imaginary component is anti-symmetric. In such pseudo-Hermitian configurations the eigenfunctions are no longer orthogonal, i.e., $\langle m|n\rangle \neq \delta_{\mathrm{mn}}$, and hence the vector space is skewed. Even more intriguing is the possibility of a sharp symmetry-breaking transition once a non-Hermiticity parameter exceeds a certain critical value [28]. In this latter regime, the Hamiltonian and the PT operator no

1077-260X © 2016 IEEE. Personal use is permitted, but republication/redistribution requires IEEE permission.
See http://www.ieee.org/publications_standards/publications/rights/index.html for more information.

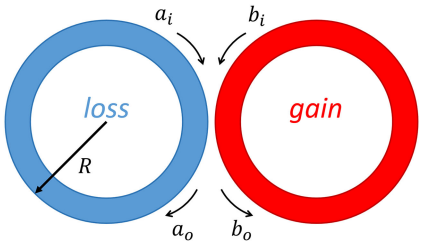


Fig. 1. Schematic of a PT-symmetric coupled microring arrangement.

longer display the same set of eigenfunctions (even though they commute) and as a result the eigenvalues of the system cease to be entirely real. In addition, this broken PT-symmetry phase is associated with the appearance of the so-called exceptional points [29].

Later, it was shown that photonics can provide a fertile ground where PT-symmetry concepts can be experimentally investigated and utilized [8], [9]. The transition from quantum mechanics to optics can be formally justified by considering the isomorphism between the Schrödinger and the optical wave equations. In this regard, the complex refractive index profile plays the role of an optical potential, i.e. $V(x) = k_0(n_R(x) + in_I(x))$. In optical systems, PT-symmetry demands that the spatial distribution of the refractive index is an even function $(n_R(x) = n_R(-x))$, whereas the imaginary component (representing gain or loss) is an odd function of position $(n_I(x) = -n_I(-x))$ [8].

## III. PT-Symmetric Coupled Microring Resonators

Coupled micro-resonators provide a viable platform to explore the physics and applications of parity-time symmetry in optics [7], [20], [21]. In a coupled microcavity arrangement, PT-symmetry can be held if one resonator is subject to gain while the other experiences an equal amount of loss. A schematic representing such a dual cavity structure is depicted in Fig. 1 in which two identical transversely-single-mode resonators of radius *R*, are evanescently coupled to each other. The field distribution in the two rings can then be described via a system of spatial coupled mode equations. Here, we assume that the coupling strength is approximately constant over the short coupling distance, where the two ring resonators are in close proximity of each other- locally it may be treated as a phase-matched directional coupler. The modal amplitudes in the two cavities (*a(z)* and *b(z)*) are governed by the following relations:

$$\begin{cases} a_o = a_i\cos(\theta) + ib_i\sin(\theta) \\ b_o = ia_i\sin(\theta) + b_i\cos(\theta), \end{cases} \tag{1}$$

where $\theta = \kappa_s l_{\text{eff}}$ represents the coupling angle, $l_{\text{eff}}$ is the effective length of the coupler, and $\kappa_s$ represents the spatial coupling constant. Similarly, light propagation in the closed path of the two resonators demands that:

$$\begin{cases} a_i = a_o\exp(i\phi - g) \\ b_i = b_o\exp(i\phi + g), \end{cases} \tag{2}$$

where $g$ is the amplification/attenuation in the rings per roundtrip, and $\phi$ is the complex phase. Using (1) and (2), one can show that:

$$\begin{pmatrix} -1 + \exp(i\phi - g)\cos(\theta) & i\exp(i\phi + g)\sin(\theta) \\ i\exp(i\phi - g)\sin(\theta) & -1 + \exp(i\phi + g)\cos(\theta) \end{pmatrix} \times \begin{pmatrix} a_o \\ b_o \end{pmatrix} = 0. \tag{3}$$

In order for this system to have nontrivial solutions, the determinant of the matrix in Eq. (3) should be equal to zero:

$$\cos(\phi) = \cos(\theta)\cosh(g). \tag{4}$$

Given that $\phi$ is directly proportional to the resonance frequencies, the above equation can be solved to find the complex eigenfrequencies of the system. Considering that $\theta$ and $g$ are small parameters, one can then find $\phi$ in terms of the gain/loss and coupling coefficients:

$$\phi_m = 2m\pi \pm \sqrt{\theta^2 - g_m^2}, \tag{5}$$

where the subscript *m* represents different longitudinal modes. While the coupling strength $(\theta)$ remains almost the same for the neighboring longitudinal modes due to their identical mode profile, the amount of gain for each mode may vary substantially following the lineshape function of the active medium. In general, depending on the relative strength of coupling and gain, $\phi$ can assume complex values. The real part of $\phi$ represents the resonance frequencies, while the imaginary component expresses the amplification (positive) or decay (negative) rate associated with the modal fields. Equation (5) reveals that if the level of gain/loss remains below the coupling coefficient $(\theta > g_m)$, the two supermodes (with split resonant frequencies) undergo neutral oscillations (neither of them experiences attenuation or amplification). On the other hand, as soon as the gain/loss contrast exceeds the coupling coefficient $(\theta < g_m)$, a conjugate pair of lasing/decaying modes emerges. This transition point is called the PT-symmetry breaking threshold or the exceptional point. Of interest is to design a laser system in such a way that only the longitudinal mode with the highest amount of gain operates beyond the PT-symmetry breaking, while all other longitudinal modes remain below this threshold. In such a setting, lasing occurs only in the designated longitudinal mode, with considerably enhanced mode discrimination due to the presence of an exceptional point [7]. This enables single mode operation at pump levels well above threshold, where an ordinary single microring laser will be fully multi-moded.

## IV. Threshold Analysis for PT-Symmetric Lasers

In this Section, the lasing threshold condition for a PT-symmetric microring arrangement will be derived by taking into account gain saturation. The effect of an exceptional point on the threshold of a non-uniformly pumped dual cavity laser system was also analyzed in previous studies [23], [30]. Here, we use temporal coupled mode equations that describe the time evolution of the modal fields for the *m*th longitudinal mode in

the active cavity ($E_{1m}$) and in the lossy resonator ($E_{2m}$):

$$\frac{dE_{1m}}{dt} = -\gamma E_{1m} + \frac{\sigma(p-1)}{1+\varepsilon|E_{1m}|^2}E_{1m} + i\kappa E_{2m} \quad (6a)$$

$$\frac{dE_{2m}}{dt} = -\gamma E_{2m} - \frac{\sigma}{1+\varepsilon|E_{2m}|^2}E_{2m} + i\kappa E_{1m}. \quad (6b)$$

Here, $\kappa$ denotes a temporal coupling coefficient between these two cavities, and it is related to the spatial coupling $\theta$ described above through $\kappa = \theta v_g/(2\pi R)$, where $v_g$ is the group velocity, and R is the radius of the ring resonator. The linear loss $\gamma$ (scattering, radiation losses, out-coupling, *etc*.) is taken to be the same in both resonators and it relates to quality factor Q via $\gamma = c/(\lambda_0\, Q)$. In these equations $\sigma(p\text{-}1)$ and $\sigma$ respectively represent the small signal gain (for $p>1$) due to the pumping parameter $p$ of the quantum wells and absorption loss in the absence of pumping, where $\sigma = \Gamma v_g A N_0$, with *A* being the gain constant, $N_0$ the transparency carrier population density, and $\Gamma$ the confinement factor. Moreover, $p = \tau_e R_p/N_0$ is the pump parameter, where the carrier generation rate is given by $R_p = \eta I/(\hbar\omega_p d)$ and *I*, $\eta$, *d* represent the pump intensity, external quantum efficiency, and the height of the multiple quantum wells in each micro-ring, respectively. In addition, $\tau_e$ is the carrier lifetime and $\hbar\omega_{\rm p}$ is the energy of a pump photon. The parameter $\varepsilon$ is inversely proportional to the saturation intensity $\varepsilon = nc\tau_e \in_0 A\Gamma/(2\hbar\omega)$, where *n* is the refractive index of the structure [31]. We note that, in the weak coupling regime, the temporal analysis presented here is equivalent to the spatial formalism used in Section III.

To find the lasing threshold, the above equations are first linearized (small field amplitudes). In this respect, the nonlinearities have no effect on the threshold conditions of this system. Nevertheless, they play a crucial role in determining its steady state response. By adopting the parameters $G_m = \sigma(p-1)$ and $(a_m, b_m) = \sqrt{\varepsilon}(E_{1m}, E_{2m})$, we arrive at:

$$\frac{da_m}{dt} = -\gamma a_m + G_m a_m + i\kappa b_m \quad (7a)$$

$$\frac{db_m}{dt} = -\gamma b_m - \sigma b_m + i\kappa b_m. \quad (7b)$$

In the linearized region, the eigenvalues of this system, $\xi$, can be obtained through $(a_m, b_m) = (a_{0m}, b_{0m})exp(-i\xi t)$, where $a_{0m}$ and $b_{0m}$ are in general complex constants. Hereby, two regimes can be identified, depending on the value of $(G_m+\sigma)$. In the first case, where $(G_m+\sigma) < 2\kappa$, the modal solutions of Eqs. (7a) and (7b) are associated with the symmetry-preserved case and are given by,

$$\begin{pmatrix} a_m \\ b_m \end{pmatrix} = \begin{pmatrix} 1 \\ \pm\exp(\pm i\delta) \end{pmatrix} \exp\left(\frac{G_m-\gamma}{2} - \gamma\right) \times \exp(\pm i(\kappa\cos(\delta)t)), \quad (8)$$

where $\sin(\delta) = (G_m+\sigma)/2\kappa$. If on the other hand, $(G_m+\sigma) > 2\kappa$, the solutions are given by:

$$\begin{pmatrix} a_m \\ b_m \end{pmatrix} = \begin{pmatrix} 1 \\ i\exp(\pm i\delta) \end{pmatrix} \exp\left(\frac{G_m-\gamma}{2} - \gamma\right) \times \exp(\mp\kappa(\sinh(\delta)t)), \quad (9)$$

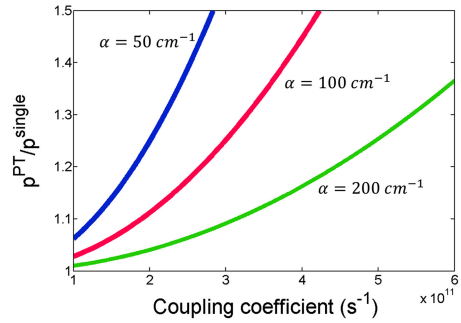


Fig. 2. Ratio of lasing thresholds for PT-symmetric arrangement to single microring, at different coupling coefficients and for various absorptions in the quantum wells.

where $\cosh(\delta) = (G_m+\sigma)/2\kappa$. These latter solutions are characteristics of a broken PT-symmetry phase, since the fields in the two cavities are now unequal. If the system operates in the unbroken PT-symmetry regime, given by Eq. (8), then, according to the exponential term, linear amplification takes place if the gain is above the total loss in the system, *i.e.* $G_m > (2\gamma+\sigma)$. However, in the broken PT-symmetric phase, Eq. (9), growth occurs if $G_m > \kappa^2(\gamma+\sigma)^{-1} + \gamma$. To derive this latter condition, one has to consider the $\kappa(\sinh(\delta))$ term in the exponent. From these two threshold conditions, it can be directly inferred that if $(\gamma+\sigma)>\kappa$, then the PT-broken phase has a lower threshold and hence is the one to lase. Conversely, if $(\gamma+\sigma)<\kappa$, the situation is reversed and the unbroken PT eigenstate will be the one to experience amplification. These two lasing thresholds can be summarized by the following relationship [30]

$$G_{\rm th} = \min\left[\gamma + \frac{\kappa^2}{\gamma+\sigma}, 2\gamma+\sigma\right]. \quad (10)$$

To contrast these results to the lasing threshold of a single ring, one should consider the field dynamics described by Eq. (7a) in the absence of coupling ($\kappa = 0$). In this case, the lasing threshold is simply given by $G_m^{\rm th} = \gamma$ [30]. A typical set of parameter values in such semiconductor quantum well structures can provide a good comparison between a single ring and a PT-symmetric laser arrangement. Assuming $Q$ = 120,000, hence the photon decay rate at $\lambda = 1.55$ $\mu$m is $\gamma = 1.5\times10^9\ s^{-1}$. The unsaturated absorption loss $\sigma$ for $\Gamma = 0.5$, $v_g = c/3.8$, A = 2 $\times$ $10^{-20}$ m$^2$ and $N_0 = 10^{24}$ m$^{-3}$, is estimated to be $\sigma = 8\times10^{11}\ s^{-1}$. The coupling $\kappa$ can be determined from the splitting of the longitudinal modes i.e. $\Delta\omega = 2\kappa$. From our experiments, we find that $\kappa$ is in the order of $4\times10^{11}\ s^{-1}$ [32]. These values clearly indicate that $(\gamma+\sigma)>\kappa$ and therefore lasing in our structure is initiated in the broken symmetry mode. In this case, the threshold pump parameter for the PT-symmetric case is given by:

$$p^{\rm PT} = 1 + \frac{\gamma}{\sigma} + \frac{\kappa^2}{\sigma(\gamma+\sigma)}. \quad (11)$$

In comparison, the lasing threshold for a single ring is $p^{\rm single} = 1 + (\gamma/\sigma)$. Given that for the aforementioned values, $\gamma << \kappa < \sigma$, one can arrive at the interesting conclusion that these two thresholds are fairly close to each other. Fig. 2 illustrates

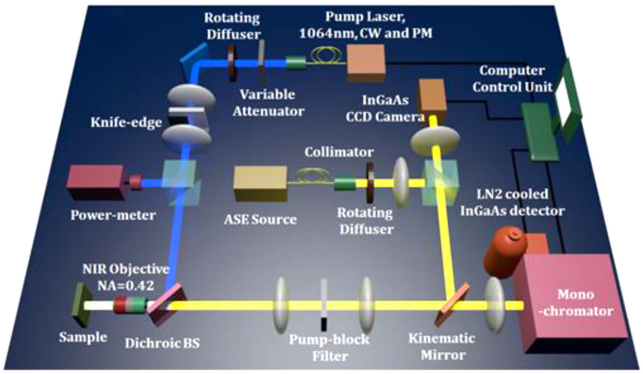


(a)

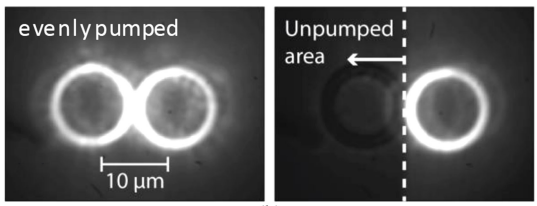


(b)

Fig. 3. (a) Schematic of a micro-photoluminescence characterization set-up (b) A knife edge is used to selectively withhold pump from one of the rings.

the ratio $p^{\mathrm{PT}}/p^{\mathrm{single}}$ as function of the coupling strength when unsaturated absorption in the quantum well cavities is varying from 50 to 200 $\mathrm{cm}^{-1}$.

The pump intensity corresponding to these values of pump parameter ($p$) can be obtained from the relation $I = (\hbar\omega_p dpN_0)/(\eta\tau_e)$. Assuming a quantum efficiency of $\eta\sim0.5$, an active layer depth of 210 nm and a typical carrier lifetime of 4 ns, the incident pump intensity required for the PT symmetric configuration to lase is $I \sim 2.5 \times 10^3$ $\mathrm{Wcm}^{-2}$, provided that $p^{\mathrm{PT}} \sim 1.2$. In our experiment, the threshold pump intensity was measured to be approximately $I \sim 2.7 \times 10^3$ $\mathrm{Wcm}^2$ in excellent agreement with theoretical estimates.

## V. Sample Fabrication and Measurement Setup

The microring resonators are fabricated using standard nano-fabrication techniques. The gain region is comprised of six quantum wells of $\mathrm{In_{x=0.56}Ga_{1-x}}As_{\mathrm{y=0.938}}\mathrm{P_{1-y}}$ (10 nm) $/\mathrm{In_{x=0.734}Ga_{1-x}As_{y=0.57}P_{1-y}}$ (20 nm) covered with an InP film (10 nm) for protection. The overall height of the active layer is 210 nm and the quantum wells are grown on a p-type InP substrate. The microring patterns are then defined on the wafer by high-resolution electron beam lithography. The patterns are transferred to the active region by a reactive ion etching process utilizing $H_2$:$CH_4$:Ar (40:4:20 sccm). After oxygen plasma cleaning of the sample, 3 $\mu$m of a $SiO_2$ (silicon dioxide) is deposited using PECVD (plasma-enhanced chemical vapor deposition). Next, the wafer is flipped and bonded to a glass mount using SU8 photoresist. This allows the InP substrate to be completely removed by dipping the sample in HCl (Hydrochloric acid). The final patterns are InGaAsP exposed rings that partially buried in $SiO_2$ [7].

For the characterization of the PT microring lasers, we used a micro-luminescence characterization setup shown schematically in Fig. 3(a). The pump beam (1064 nm laser with pulse duration of 15 ns and a repetition rate of 290 kHz) is projected to the sample via an NIR objective with a numerical aperture of 0.42. The pump beam is shaped such that it uniformly illuminates a circular area on the surface of the sample with a diameter of 80 $\mu$m. In order to selectively block certain areas from pump illumination we utilize a knife-edge as shown in Fig. 3(b). The location of the knife-edge is controlled by a translation stage while the location of its shadow on the sample plane is monitored via a confocal microscope. In this manner, different scenarios of evenly pumped and PT-symmetric schemes can be realized. The objective lens also collects the emitted power from the microring lasers and directs it onto either an infrared CCD camera, or the entrance slit of a spectrograph attached to a LN2 cooled InGaAs detector, each by using a pair of two cascaded 4f imaging systems. All spectra reported in this manuscript are recorded with a resolution of $\sim$0.4 nm [32].

## VI. Experimental Results

The emission spectra from a single microring, evenly pumped coupled rings, as well as PT-symmetric microring system are shown in Fig. 4. Here, each microring has a radius of 10 $\mu$m, a width of 500 nm, and a depth of 210 nm. These dimensions are chosen to ensure single transverse mode operation ($\mathrm{TE}_0$). The separation between the coupled rings is 150 nm. As is evident in the spectrum of a single ring illustrated in Fig. 4(a), this laser supports the concurrent oscillation of multiple longitudinal modes. In Fig. 4(b) also, when two adjacent coupled rings are pumped evenly, the coupling introduces a splitting in the longitudinal resonances without significantly affecting their modal discrimination. On the contrary, in the PT symmetric laser of Fig. 4(c) where one resonator experiences gain and the other loss, only the mode with the highest gain oscillates. In this regime, the laser operates in a single mode fashion with a side-lobe suppression ratio of $\sim$30 dB. Fig. 5 shows the emission intensities collected from the scattering off the ring surfaces. Clearly, when both rings are pumped, the supermodes are distributed equally between the two resonators (Fig. 5(a)). On the other hand, in the PT arrangement, the lasing mode primarily resides in the pumped cavity (Fig. 5(b)). As a result, it is expected that the efficiency of the dominant lasing mode in the PT configuration not to be compromised by the presence of the lossy cavity as long as it operates in the broken symmetry regime. This is also evident from the slope efficiency of the light-light plots for the single ring and PT-symmetric arrangement presented in Fig. 6. Here, the slope efficiency, associated to the total output power in all modes, is approximately the same in both lasers, despite the fact that in the PT case a lossy resonator is involved. It should also be noted that in Fig. 6(b) the reported output power is distributed between several spectral lines, while in Fig. 6(a) the power emits into one single mode.

## VII. Deviations From Perfect PT-Symmetry

The analysis in Section III assumes perfect PT-symmetric conditions, *i.e.*, two entirely identical rings exhibiting equal amounts of gain and loss. In practice, however, it may not

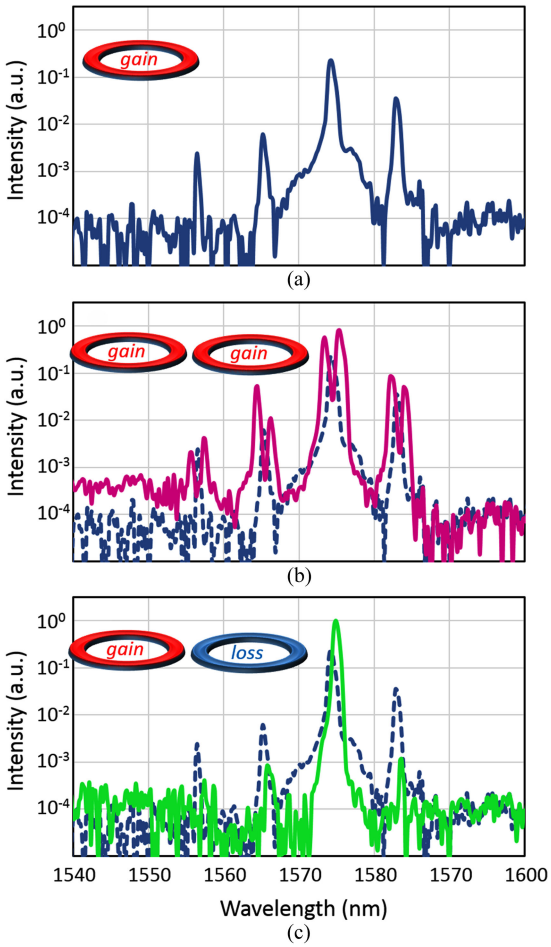


Fig. 4. Emission spectra of (a) single isolated microring laser: multiple longitudinal modes are lasing within the gain bandwidth. (b) Two coupled active microrings: the degeneracy of each mode breaks and the resonance wavelengths split into two. (c) PT symmetric microring laser arrangement: single mode operation is enforced with side mode suppression ratio of ∼30 dB. If pumped, each ring is subjected to ∼0.5 mW of power.

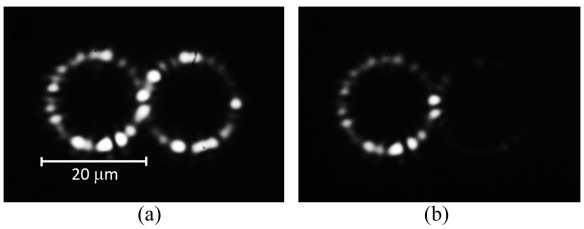


Fig. 5. Intensity profiles collected through scattering off the samples. (a) Evenly pumped microrings: the suppermodes circulate in both rings (b) a PT symmetric microring arrangement: the mode resides exclusively within the gain cavity.

always be possible to fulfill these conditions. To begin with, even if PT-symmetry is exactly held for one pair of modes, the wavelength dependence of the gain medium as well as the bending and scattering losses may cause deviations from this condition for the rest of the modes. In addition, due to the interdependence of refractive index and gain/loss (Kramers-Kronig relations), even structurally identical ring resonators can be detuned when being subjected to different pump energies. Yet,

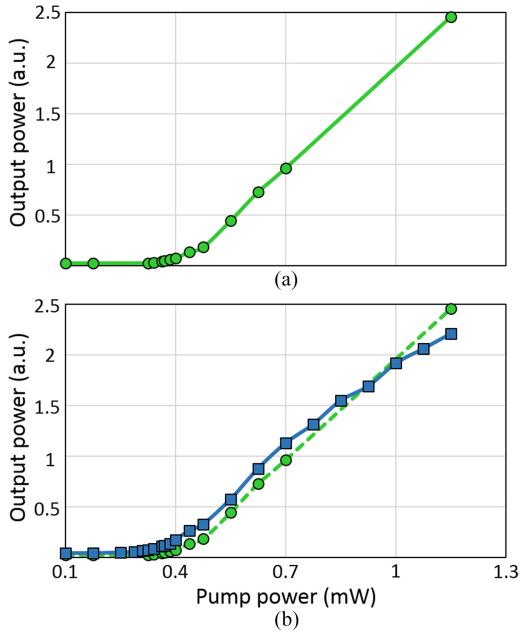


Fig. 6. The light-light curve for (a) a PT-symmetric coupled microring laser and (b) an isolated microring laser (blue solid line) compared to that of the PT laser (green dashed line). The slope efficiency of the PT arrangement is not deteriorated by the presence of the lossy resonator. The rings have a radius of 5 $\mu$m, a width of 500 nm, and depths of 210 nm, also separation between the rings in the PT configuration is 200 nm.

as we will show in this Section, the strong coupling between the ring resonators makes the PT-symmetric mode selection technique resilient to some level of perturbation. To study this problem in a systematic way, we formulate a situation where the gain/loss and the resonant frequencies in the two coupled resonators are not exactly equal. Here, the radii and the loss/gain parameters associated with the two rings are denoted as $R_{1,2}$ and $g_{1,2}$, respectively. Following an approach similar to that outlined in Section III, we find the following self-consistent relationship between the fields in the two resonators ($a$ and $b$):

$$\begin{pmatrix} -1+\exp(i\phi_1-g_1)\cos(\theta) & i\exp(i\phi_2+g_2)\sin(\theta) \\ i\exp(i\phi_1-g_1)\sin(\theta) & -1+\exp(i\phi_2+g_2)\cos(\theta) \end{pmatrix} \times \begin{pmatrix} a_o \\ b_o \end{pmatrix} = 0, \quad (12)$$

where as before $\theta$ represents the coupling strength, and $\phi_1$, $\phi_2$ describe complex phase accumulation per roundtrip in the two cavities. In order for this system to have nontrivial solutions, the determinant of the matrix in Eq. (12) must be equal to zero:

$$1+\exp(i\,(\phi_1+\phi_2))\exp(g_2-g_1)-\cos(\theta)\cdot\exp(i\phi_1) \times\exp(-g_1)\,(1+\exp(i\,(\phi_2-\phi_1)\exp(g_2+g_1))=0. \quad (13)$$

Note that if caused by perturbations, it is generally expected that the mismatch between the resonant frequencies of the rings to be small, therefore one can assume $\phi_2=\phi_1+\Delta\phi$, where $\Delta\phi \ll \phi_{1,2}$. On the other hand, the gain and loss can, in practice, significantly deviate from their exact PT balance. This is due to fact that the loss of the un-pumped ring is dictated by the

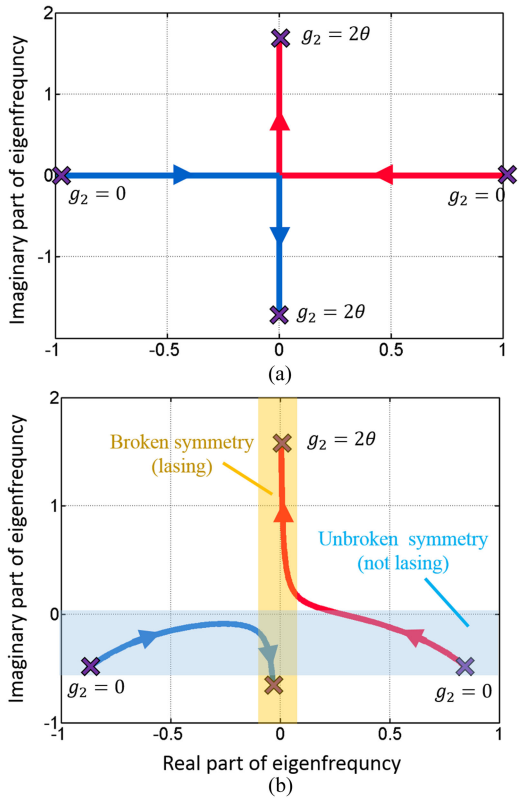


Fig. 7. The real and imaginary parts of the normalized eigenfrequencies associated with (a) a perfectly PT-symmetric, and (b) a perturbed PT-symmetric coupled microring arrangements, where the gain in the active ring is varied from 0 to $2\theta$. The loss in the un-pumped resonator $g_1$, and the phase mismatch $\Delta\phi$ are set to be $\theta$ and $0.03\theta$, respectively. In the perturbed PT system, the general trends remain the same as long as the two rings are strongly coupled.

absorption and scattering, while the gain in the pumped cavity can attain a wide range of values depending on the intensity of the pump. Considering the above, Eq. (13) can be solved to find the eigenfrequency of the *m*th longitudinal mode:

$$\phi_{m1,2} = 2m\pi + \frac{\Delta\phi}{2} + i\frac{g_2 - g_1}{2} \pm \sqrt{\theta^2 - \left(\frac{g_1 + g_2}{2} + i\frac{\Delta\phi}{2}\right)^2}. \quad (14)$$

In order to visually illustrate how the system responds to deviations, the evolution of eigenfrequencies, when the gain in the active ring changes from 0 to $2\theta$, are plotted in the complex plane for a double ring structure under perfect PT-symmetric conditions (Fig. 7(a)), and the same system subject to the above perturbations (Fig. 7(b)). As shown in Fig. 7(b), for the perturbed system, the eigenfrequencies are of a complex nature and the transition from the unbroken to the broken regime occurs in a more adiabatic fashion. This effect has also been observed in previous experimental studies concerning photonic molecule lasers [26]. However, regardless of these differences, as long as the deviations are well below the level required to fully decouple the two rings (perhaps 10% of the coupling), the overall behavior of the modes remains the same. Therefore, by using strongly coupled resonators as demonstrated in this work, it is possible to achieve robust single mode operation despite small perturbations due to fabrication imperfections or pump-induced nonlinearities.

## VIII. Conclusion

In conclusion, we have demonstrated that the exceptional points in PT-symmetric configurations can be effectively utilized for mode management in semiconductor microring laser arrangements. In our system, PT-symmetry is realized by pairing an active microring resonator with an identical but lossy partner. This configuration operates in a stable single mode fashion without compromising the threshold pump level, slope efficiency, and output power. Our analysis indicates that this mechanism of mode selectivity is robust with respect to fabrication errors, and is by nature broadband and self-adaptive. Our results may pave the way for a new class of compact semiconductor lasers based on the physics of non-Hermitian exceptional points.

## References

[1] O. Svelto, *Principles of Lasers*, D. C. Hanna, Ed. New York, NY, USA: Springer, 1976.
[2] W. T. Tsang, N. A. Olsson, R. A. Linke, and R. A. Logan, "1.5 $\mu$m wavelength GaInAsP C3 lasers: Single-frequency operation and wideband frequency tuning," *Electron. Lett.*, vol. 19, no. 11, pp. 415–417, 1983.
[3] L. Coldren and T. L. Koch, "Analysis and design of coupled-cavity lasers—Part I: Threshold gain analysis and design guidelines," *IEEE J. Quantum Electron.*, vol. QE-20, no. 6, pp. 659–670, Jun. 1984.
[4] J. E. Carroll, J. Whiteaway, and D. Plumb, *Distributed Feedback Semiconductor Lasers*. Stevenage, U.K.: Inst. Eng. Technol., 1998.
[5] J. C. Hulme, J. K. Doylend, and J. E. Bowers, "Widely tunable Vernier ring laser on hybrid silicon," *Opt. Exp.*, vol. 21, no. 17, pp. 19718–19722, 2013.
[6] K. J. Vahala, "Optical microcavities," *Nature*, vol. 424, no. 6950, pp. 839–846, 2003.
[7] H. Hodaei, M.-A. Miri, M. Heinrich, D. N. Christodoulides, and M. Khajavikhan, "Parity-time–symmetric microring lasers," *Science*, vol. 346, no. 6212, pp. 975–978, 2014.
[8] K. G. Makris, R. El-Ganainy, D. N. Christodoulides, and Z. H. Musslimani, "Beam dynamics in P T symmetric optical lattices," *Phys. Rev. Lett.*, vol. 100, no. 10, art. no. 103904, 2008.
[9] R. El-Ganainy, K. G. Makris, D. N. Christodoulides, and Z. H. Musslimani, "Theory of coupled optical PT-symmetric structures," *Opt. Lett.*, vol. 32, no. 17, pp. 2632–2634, 2007.
[10] S. Longhi, "Bloch oscillations in complex crystals with P T symmetry," *Phys. Rev. Lett.*, vol. 103, no. 12, art. no. 123601, 2009.
[11] A. Guo *et al.*, "Observation of P T-symmetry breaking in complex optical potentials," *Phys. Rev. Lett.*, vol. 103, no. 9, art. no. 093902, 2009.
[12] C. E. Rüter *et al.*, "Observation of parity–time symmetry in optics," *Nat. Phys.*, vol. 6, no. 3, pp. 192–195, 2010.
[13] A. Regensburger *et al.*, "Parity-time synthetic photonic lattices," *Nature*, vol. 488, no. 7410, pp. 167–171, 2012.
[14] S. Longhi, "PT-symmetric laser absorber," *Phys. Rev. A*, vol. 82, no. 3, art. no. 031801, 2010.
[15] Y. D. Chong, L. Ge, and A. D. Stone, "PT-symmetry breaking and laser-absorber modes in optical scattering systems," *Phys. Rev. Lett.*, vol. 106, no. 9, art. no. 093902, 2011.
[16] A. Szameit, M. C. Rechtsman, O. Bahat-Treidel, and M. Segev, "PT-symmetry in honeycomb photonic lattices," *Phys. Rev. A*, vol. 84, no. 2, art. no. 021806, 2011.
[17] A. E. Miroshnichenko, B. A. Malomed, and Y. S. Kivshar, "Nonlinearly PT-symmetric systems: Spontaneous symmetry breaking and transmission resonances," *Phys. Rev. A*, vol. 84, no. 1, art. no. 012123, 2011.
[18] E. M. Graefe and H. F. Jones, "PT-symmetric sinusoidal optical lattices at the symmetry-breaking threshold," *Phys. Rev. A*, vol. 84, no. 1, art. no. 013818, 2011.

[19] L. Feng *et al.*, "Experimental demonstration of a unidirectional reflectionless parity-time metamaterial at optical frequencies," *Nat. Mater.*, vol. 12, no. 2, pp. 108–113, 2013.
[20] B. Peng *et al.*, "Parity-time-symmetric whispering-gallery microcavities," *Nat. Phys.*, vol. 10, no. 5, pp. 394–398, 2014.
[21] L. Chang *et al.*, "Parity-time symmetry and variable optical isolation in active-passive-coupled microresonators," *Nat. Photon.*, vol. 8, no. 7, pp. 524–529, 2014.
[22] M.-A. Miri, P. LiKamWa, and D. N. Christodoulides, "Large area single-mode parity–time-symmetric laser amplifiers," *Opt. Lett.*, vol. 37, no. 5, pp. 764–766, 2012.
[23] M. Liertzer *et al.*, "Pump-induced exceptional points in lasers," *Phys. Rev. Lett.*, vol. 108, no. 17, art. no. 173901, 2008.
[24] M. Kulishov and B. Kress, "Distributed bragg reflector structures based on PT-symmetric coupling with lowest possible lasing threshold," *Opt. Exp.*, vol. 21, no. 19, pp. 22327–22337, 2013.
[25] L. Feng, Z. J. Wong, R. M. Ma, Y. Wang, and X. Zhang, "Single-mode laser by parity-time symmetry breaking," *Science*, vol. 346, no. 6212, pp. 972–975, 2014.
[26] M. Brandstetter *et al.*, "Reversing the pump dependence of a laser at an exceptional point," *Nat. Commun.*, vol. 5, art. no. 4034, 2014.
[27] B. Peng *et al.*, "Loss-induced suppression and revival of lasing," *Science*, vol. 346, no. 6207, pp. 328–332, 2014.
[28] C. M. Bender and S. Boettcher, "Real spectra in non-Hermitian Hamiltonians having PT symmetry," *Phys. Rev. Lett.*, vol. 80, no. 24, art. no. 5243, 1998.
[29] S. Klaiman, U. Günther, and N. Moiseyev, "Visualization of branch points in PT-symmetric waveguides," *Phys. Rev. Lett.*, vol. 101, no. 8, art. no. 080402, 2008.
[30] A. U. Hassan, H. Hodaei, M.-A. Miri, M. Khajavikhan, and D. N. Christodoulides, "Nonlinear reversal of the PT-symmetric phase transition in a system of coupled semiconductor microring resonators," *Phys. Rev. A*, vol. 92, no. 6, art. no. 063807, 2015.
[31] E. A. Ultanir, D. Michaelis, F. Lederer, and G. I. Stegeman, "Stable spatial solitons in semiconductor optical amplifiers," *Opt. Lett.*, vol. 28, no. 4, pp. 251–253, 2003.
[32] H. Hodaei *et al.*, "Parity-time-symmetric coupled microring lasers operating around an exceptional point," *Opt. Lett.*, vol. 40, no. 21, pp. 4955–4958, 2015.

**Hossein Hodaei** received the B.Sc. degree from the Isfahan University of Technology, Isfahan, Iran, in 2011, and the M.Sc. degree in electrical engineering from the Sharif University of Technology, Tehran, Iran, in 2013. He is currently working toward the Ph.D. degree in the Plasmonics and Applied Quantum Optics Group, College of Optics and Photonics, University of Central Florida, Orlando, FL, USA.

His research interests include parity-time symmetry, novel semiconductor lasers, and non-Hermitian optics.

**Absar U. Hassan** received the B.Sc. degree in electrical engineering from the School of Science and Engineering, Lahore University of Management Sciences, Lahore, Pakistan, in 2013. Since Fall 2013, he has been working toward the Ph.D. degree in optics having joined the Nonlinear Waves Group under the supervision of Dr. Demetrios N. Christodoulides, at the College of Optics and Photonics, University of Central Florida, Orlando, FL, USA. His research interests include non-Hermitian optics and solitary-waves in photonic systems.

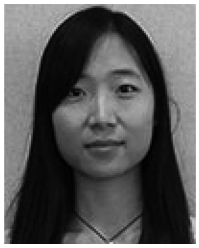

**Jinhan Ren** was born in Hebei, China, on November 24, 1990. She received the B.S. and M.S. degrees in electrical engineering from the Harbin Institute of Technology, Harbin, China, in 2012 and 2014, respectively. She is currently working toward the Ph.D. degree in the Plasmonics and Applied Quantum Optics Laboratory, College of Optics and Photonics, University of Central Florida, Orlando, FL, USA.

**William E. Hayenga** received the B.Sc. degree in physics from Iowa State University, Ames, IA, USA, in 2012. He is currently working toward the Ph.D. degree in the Plasmonics and Applied Quantum Optics Group, College of Optics and Photonics, University of Central Florida, Orlando, FL, USA. His research interests include plasmonic nanolasers, parity-time symmetry, and novel semiconductor lasers.

**Mohammad-Ali Miri** received the B.Sc. degree from Shiraz University, Shiraz, Iran, in 2008, and the M.Sc. degree from the Sharif University of Technology, Tehran, Iran, in 2010, both in electrical engineering, and the Ph.D. degree from the College of Optics and Photonics, University of Central Florida, Orlando, FL, USA. He has worked on general areas of non-Hermitian physics, nonlinear optics, and periodic structures. In particular, he has made contributions to the development of the newly emerging field of PT-symmetric optics. He has authored and coauthored more than 50 publications in peer-reviewed journals and conferences.

**Demetrios N. Christodoulides** received the Ph.D. degree from Johns Hopkins University, Baltimore, MD, USA, in 1986, and he subsequently joined Bellcore, Murray Hill, NY, USA, as a Postdoctoral Fellow. Between 1988 and 2002, he was with the Faculty of the Department of Electrical Engineering, Lehigh University. He is currently the Cobb Family Endowed Chair and the Pegasus Professor of optics at the College of Optics and Photonics, University of Central Florida, Orlando, FL, USA. His research interests include linear and nonlinear optical beam interactions, synthetic optical materials, optical solitons, and quantum electronics. His research initiated new innovation within the field, including the discovery of optical discrete solitons, Bragg and vector solitons in fibers, nonlinear surface waves, and the discovery of self-accelerating optical (airy) beams. He has authored and co-authored more than 300 papers. He is a Fellow of the Optical Society of America (OSA) and the American Physical Society. In 2011, he received the R.W. Wood Prize of OSA.

**Mercedeh Khajavikhan** received the B.S. and M.S. degrees in electronics from the Amirkabir University of Technology, Tehran, Iran, in 2000 and 2003, respectively, and the Ph.D. degree in electrical engineering from the University of Minnesota, Minneapolis, MN, USA, in 2009. Her Ph.D. dissertation was on coherent beam combining for high-power laser applications. In 2009, she joined the University of California in San Diego as a Postdoctoral Researcher where she worked on the design and development of nanolasers, plasmonic devices, and silicon photonics components. In August 2012, she joined the College of Optics and Photonics, University of Central Florida, Orlando, FL, USA, as an Assistant Professor. In 2015, she received the NSF Early Career Award.